# Mechanism of quasionedimensional electronic conductivity in discotic liquid crystals

N. Boden, R. J. Bushby, and J. Clements

Citation: J. Chem. Phys. **98**, 5920 (1993); doi: 10.1063/1.464886
View online: http://dx.doi.org/10.1063/1.464886
View Table of Contents: http://jcp.aip.org/resource/1/JCPSA6/v98/i7
Published by the American Institute of Physics.

# Mechanism of quasi-one-dimensional electronic conductivity in discotic liquid crystals

N. Boden, R. J. Bushby, and J. Clements
*School of Chemistry, The University of Leeds, Leeds LS2 9JT, United Kingdom*

(Received 23 November 1992; accepted 18 December 1992)

Recently, it has been shown that a new class of quasi-one-dimensional conductors can be created by doping discotic liquid crystals with appropriate oxidants. This paper reports the elucidation of the mechanism of conduction in these new materials. In particular, the ac conductivity of 2,3,6,7,10,11-hexahexyloxytriphenylene (HAT6) doped with the Lewis acid $AlCl_3$, has been measured as a function of frequency ($10^{-3}$–$10^7$ Hz), and temperature in its crystalline solid ($K$), hexagonal discotic liquid crystal ($D_{ho}$), and isotropic liquid ($I$) phases. In all three phases the conductivity is independent of frequency at low frequencies, but shows a power law dependence on frequency [$\sigma(\omega) \sim \omega^s$, $s \sim 0.7$–$0.8$] at higher frequencies. This behavior is characteristic of charge carrier transport by a hopping mechanism. The conductivity data have been analyzed in terms of the Scher and Lax theory to obtain the parameters describing this process. In macroscopically aligned $K$ and $D_{ho}$ phases, the conductivity measured along the column axes is approximately $10^3$ greater than that in the perpendicular direction. The conduction along the columns is identified with a single charge transport process in which the carriers hop between localized states (radical cations) associated with $AlCl_4^-$-counterions linearly distributed off-axis along the columns. The charge carrier diffusion coefficient is independent of the concentration of dopant and has the value $D_{\|} \sim 3.4 \times 10^{-10}$ m$^2$ s$^{-1}$ in the $D_{ho}$ phase at 343 K. In the isotropic melt phase, the conductivity measurements reveal the involvement of two distinct processes. One of these is identified with charge migration along supramolecular "stacks" some 200 nm in length, whilst the other appears to be associated with carriers hopping between these stacks. The conductivity behavior of the unaligned $D_{ho}$ and $K$ phases is very similar to that of the isotropic liquid phase implying that the mesoscopic structure of the latter phase is "frozen-in" as a "defect structure" on cooling. This defect structure then dominates the conductivity behavior of the unaligned $D_{ho}$ and $K$ phases.

## I. INTRODUCTION

One-dimensional molecular electronic conductors are of interest because of their novel physics on the one hand, and their prospects for use as *molecular wires* in molecular device applications, on the other. Many of the conducting and semiconducting organic materials which have been developed in the recent past, such as charge-transfer complexes,[1] metallo-organic complexes,[2] and doped polymers,[3] show anisotropic or quasi-one-dimensional electrical conductivity. Recently, it has been shown that a new class of one-dimensional conductors can be created by doping discotic liquid crystals with appropriate oxidants.[4–7] This paper reports the elucidation of the mechanism of conduction in these new materials. In this context, it is instructive to compare their behavior with that in related systems.

The principal structural requirement for quasi-one-dimensional conductivity is that the system possesses stacks of planar molecules or linear molecular chains along which charge transport can occur. However, stacked molecular crystal systems tend to be insulators. This is because the overlap of completely full or empty $\pi$-orbitals is weak and this leads to a band structure with a characteristically large band gap. Metalliclike conductivity has been effected by partial charge transfer to donor or acceptor molecules incorporated into the lattice: previously full (empty) orbitals are emptied (filled) enhancing orbital overlap between neighboring molecules with a concomitant reduction in the band gap.

For instance, the conductivity of neutral molecular crystals of tetracyanoquinodimethane (TCNQ) is low in contrast to that of their charge-transfer complexes with tetrathiafulvalene (TTF).[8,9] In the first case, the molecules are stacked at the van der Waals distance, the conductivity is typical of a semiconductor and the charge carrier mobility is close to $1 \times 10^{-4}$ m$^2$ V$^{-1}$ s$^{-1}$, a value typical of pure molecular crystals.[10] The charge-transfer complexes of TTF/TCNQ crystallize into segregated stacks of donors and acceptors. There is a partial transfer of electrons from TTF to TCNQ, about 0.6 e$^-$ per TTF molecule at 300 K. Conduction takes place on both columns of donors and acceptors, by holes on the TTF columns and electrons on the TCNQ columns. The conductivity is 5 S m$^{-1}$ and the carrier mobility is $3 \times 10^{-2}$ m$^2$ V$^{-1}$ s$^{-1}$ at 300 K.[11] The conduction anisotropy is about 500: however anisotropies from 30 to 30 000 have been observed[12,13] in related complexes.

Another representative group of charge-transfer complexes have been made by electrochemical oxidation of, for example, tetramethyltetraselenafulvalene (TMTSF) or tetramethyltetrathiafulvalene (TMTTF).[14] These consist of columns of TMTSF or TMTTF cations alternating with

 0021-9606/93/075920-12$06.00 

columns of inorganic or organic anions. For example, in $(TMTSF)_2X$ or $(TMTTF)_2X$, where $X$ is $PF_6$, $AsF_6$, $SbF_6$, $BF_4$ etc., each TMTSF or TMTTF molecule transfers half an electron to the $X$ column, resulting in $\frac{3}{4}$-filled bands on the cation columns and singly charged anions. Conduction is entirely on the cation columns and is therefore by holes. Typical room temperature conductivities for the $(TMTSF)_2X$ salts are 4 to 8 S $m^{-1}$, and conduction anisotropies as high as 30 000 have been observed.[1,15]

Crystalline metal complexes,[16,17] offer an alternative approach to one-dimensional conductors. Here the overlapping orbitals are generally *d-d* or *d-n*, as opposed to $\pi$-$\pi$. However, since the minimum spacing of aromatic ligands is ~0.34 nm and metal-to-metal (M-M) single bonds are generally less than 0.3 nm, these materials exhibit large band gaps and tend to be insulators.[18] When tetracyanoplatinate complexes, for instance, are doped with oxidants, electrons are removed from the top of the $d_{z^2}$ band and the antibonding nature of this bond is reduced. A strengthening of the platinum–platinum bond and associated shortening of the bond are observed. The M-M distance in untreated complexes is of the order of 0.35 nm, and the conductivities are low ($5\times10^{-9}$ S $m^{-1}$). Upon oxidation with iodine, the M-M distance decreases to 0.28 nm, only 0.003 nm longer than the value found in platinum metal.[19] The conductivity simultaneously increases to $2.3\times10^{1}$ S $m^{-1}$, and the conduction anisotropy is of the order of $10^5$.[20]

Discotic liquid crystals offer an alternative class of materials expected to show quasi-one-dimensional electronic conductivity, a prospect which has stimulated considerable interest. Their supramolecular organization and the chemical structure of the mesogens would appear to make them especially appropriate. Moreover, the combination of the electrical properties of semiconductors or conductors, with the anisotropic magnetic, optical, and mechanical properties of liquid crystals would appear to offer prospects for new applications of liquid crystals. Discotic liquid crystals are typically formed by planar molecules, with flat, conjugated cores to which are attached four or more aliphatic side chains. In the discotic columnar phases, the molecules are stacked one on top of the other in columns, which in turn, are organized on a two-dimensional lattice of either hexagonal or rectangular symmetry.[21] The intercolumnar space is occupied by highly disordered (liquidlike), insulating aliphatic side chains. The general structure of discotic liquid crystals is, therefore, very similar to that of many aromatic molecular crystals, and we can anticipate that discotics might also display quasi-one-dimensional electronic conduction.

To date, conductivity has been sought in several broad categories of discotic liquid crystals: metallomesogens,[22,23] polynuclear aromatic mesogens,[4–7] and by modification of organic charge transfer complexes.[24] Peripherally substituted metallophthalocyanines (PcM, M often Cu) display stable $D_{ho}$ columnar mesophases over extended temperature ranges.[25] The degree of *d-d* orbital overlap is small, as is the case for the crystalline analogs, and the materials are semiconducting. For example, the columnar mesophase of

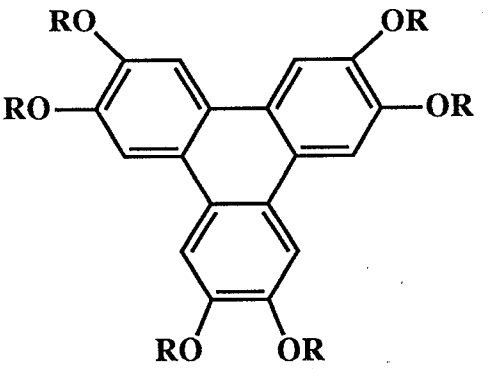


FIG. 1. The molecular structure of 2,3,6,7,10,11-hexaalkoxytriphenylene. $R$ is a normal alkyl chain, $C_nH_{2n+1}$. $n=6$ in the present work.

copper octa-*n*-octyloxyphthalocyanine has a conductivity $\sigma\sim5\times10^{-8}$ S $m^{-1}$ at 448 K. In contrast, the conductivity of the 1:1 crystalline charge transfer complex with iodine is substantially greater, $\sigma\sim3\times10^{-3}$ S $m^{-1}$. This is presumably due to an augmentation of the density of charge carriers, and a strengthening of the metal–metal bond. In the $D_{ho}$ phase of bis(octa-*n*-octadododecoxyphthalocyaninato) lutetium,[26] the conductivity is very low, $\sigma\sim10^{-12}$ S $m^{-1}$. X-ray data for the mesophases of $Pc_2Lu$ complexes, indicates a intracolumnar periodicity (M-M distance) of 0.73 nm, about twice the thickness of the phthalocyanine ring. The packing of the aromatic cores in the mesophases of these complexes clearly hinders the formation of strong metal–metal bonds, and consequently conductivities are low; moreover the conductivity is only marginally increased on oxidation with $BF_3$, $\sigma\sim10^{-10}$ S $m^{-1}$.

Charge transfer salts of highly oriented fibers of crystalline 2,3,6,7,10,11-hexapentyloxytriphenylene (HAT5), Fig. 1, have been prepared by drawing strands from the $D_{ho}$ phase followed by oxidation with bromine.[5] The conductivity of these aligned fibers ($\sigma\sim10^{-6}$ S $m^{-1}$) is three orders of magnitude greater than the corresponding powder samples ($\sigma\sim10^{-9}$ S $m^{-1}$). The electrical properties of a series of hexaalkoxytriphenylenes (HAT4, HAT5, and HAT6)[6] oxidized with approximately 70 mole% of iodine have been examined. The conductivity of thin film samples in what is believed to be the $D_{ho}$ phase was found to be $10^{-4}$–$10^{-3}$ S $m^{-1}$, but no anisotropy of the conductivity was observed. Hexahexylthiotriphenylene (HHTT)[7] displays an incommensurate helical phase in addition to the usual crystalline, columnar liquid crystalline and isotropic liquid phases, and is an insulator in its pure state ($\sigma\sim10^{-12}$ S $m^{-1}$). When oxidized with iodine to create the radical ion salt, the conductivity of thin film samples increases by approximately five orders of magnitude, but the helical phase disappears and the extent of the $D_{ho}$ phase is considerably reduced.

In all of these studies, the intention has been to prepare conducting charge transfer or radical ion salt complexes, and this has been achieved with some success, but at some expense to the mesophase behavior. We have adopted an

alternative approach.[4] We chose to dope HAT6 with *small* quantities of Lewis acids in order to preserve the essential mesophase behavior. It has been shown that doping bulk samples of HAT6 (Fig. 1, $n=6$) with 1 mole% of $AlCl_3$ converts the $D_{ho}$ phase into a quasi-one-dimensional semiconductor ($\sigma \sim 10^{-3}$ S m$^{-1}$) with the preferred direction of conductivity parallel to the axes of the columns.

To progress with the design and synthesis of conducting discotic liquid crystals we need to understand the factors governing the conductivity. To this end, in this paper we report a study of the frequency, concentration, and temperature dependence of the conductivity in aligned and unaligned samples of the HAT6/$AlCl_3$ system. In the aligned columnar phase, the conductivity is highly anisotropic and occurs by hopping of charge carriers between localized sites associated with counterions, linearly distributed along the stacks of triphenylene molecules. This anisotropy of conduction is preserved on cooling into the crystalline solid. In the isotropic melt phase, the conductivity measurements reveal the persistence of molecular stacks some 200 nm in length.

## II. MATERIALS AND METHODS

HAT6 was synthesized and purified as described previously,[27,28] and showed the following phase behavior *K* (343 K) $D_{ho}$ (374 K) *I*.

Alternating current (1 mHz–13 MHz) electrical conductivity measurements were made using both a Schlumberger–Solartron 1253 gain-phase analyzer (1 mHz to 20 kHz) and a Hewlett–Packard 4192A LF impedance analyzer (5 Hz to 13 MHz) and a sample cell with 5×5 mm platinum electrodes, coated with platinum black, separation 5 mm. In an ideal measurement cell, with parallel plates of length $l$ separated by a distance $d$, such that $l \gg d$, the electric field vector will always be perpendicular to the plane of the plates. However, when $l \approx d$ this is no longer the case. We have estimated the inhomogeneity of the electric field for the cell we have used, where $l=d$, by solving the Laplace equation with appropriate boundary conditions using a relaxation method. This has enabled us to estimate the effect of inhomogeneities on the measured conductivities. For a uniaxial mesophase, homogeneously aligned between the plates of the cell, we have estimated that inhomogeneities of the electric field lead to an underestimate of the conductivity measured perpendicular to mesophase director by about 5%, and an overestimate of the conductivity measured parallel to the mesophase director of the same order.

The cell was filled with ~1 g of pure HAT6, which was then degassed by repeated melt-pump-freeze cycles. Appropriate amounts of freshly sublimed $AlCl_3$ (mole fraction 0.005–0.05) were weighed into the cell, which was then cooled to liquid nitrogen temperatures, evacuated to $\sim 10^{-4}$ Torr and sealed. The sample was then heated into the isotropic phase at 378 K where the reaction took place: the sample was sonicated to ensure complete reaction and homogeneous dispersion of the product. The temperature of the sample was controlled to within 50 mK using a Techne TU-16D thermostat, and measured using copper/constantan thermocouples and a Keithley 181 nanovoltmeter. Samples were aligned by slowly cooling from the isotropic phase into the columnar phase in the presence of a magnetic field ($B=2.2$ T).[29]

High frequency ($f \geqslant 10^6$ Hz) ac measurements are subject to errors caused by propagation delays and phase errors introduced by the test leads. The Hewlett–Packard 4192A LF impedance analyzer has a cable length switch which facilitates balancing of the measuring bridge circuit and minimizes measurement errors when standard 1 m test leads are used. However, measurements made on high quality standard resistors at high frequencies have shown some additional reactive effects which are not compensated. These effects are also present in corresponding measurements on the HAT6/$AlCl_3$ system. These measurements have therefore been corrected using data obtained from calibration experiments on a series of standard resistors.

The phase behavior of samples was established by DSC using a Perkin–Elmer DSC2, with indium as a calibration standard. Samples were prepared by filling small glass tubes (o.d. 5 mm) with about 0.2 g of the mesogen, and repeating the procedure outlined for the preparation of samples for conductivity measurements. The tube was then broken open in a nitrogen dry box, and a small quantity, ~5 mg, transferred into a hermetically sealable DSC pan.

X-ray diffraction measurements were carried out using an INEL XRG 3000 generator, Cu $K\alpha$ radiation, a Ge(002) curved crystal monochromator, and a CPS 120 one-dimensional curved position sensitive detector. Capillary tubes (i.d. 0.5 mm), were filled with some of the material prepared for DSC measurements, flame sealed, and mounted into a chamber, whose temperature was controlled and measured to within 0.5 K.

## III. RESULTS

### A. Phase behavior and structure

The pure mesogen was found by DSC to have the following phase behavior, *K* (343 K) $D_{ho}$ (374 K) *I* [Lit.[30] *K* (341 K) $D_{ho}$ (372 K) *I*]. On doping with $AlCl_3$ the transition temperatures are depressed, and the transitions become biphasic, Fig. 2. The upper and lower boundaries of the biphasic regions are seen to vary fairly linearly with the concentration of $AlCl_3$ (mole fraction $x$), a Henry's law type behavior.[31] We believe the reaction involved is

$$3\mathrm{HAT6} + 4\mathrm{AlCl_3} \rightarrow 3(\mathrm{HAT6}^{\cdot +}\mathrm{AlCl_4^-}) + \mathrm{Al}, \qquad (1)$$

so that the concentration of ($HAT6^{\cdot +}AlCl_4^-$), the radical salt formed in the reaction, is $0.75x$.[32] Thus the observed behavior suggests that we can consider the doped system as equivalent to HAT6 into which the radical salt is incorporated as a solute. Whilst we might expect the incorporation of $HAT6^{\cdot +}$ into the triphenylene columns to enhance the transition temperatures, incorporation of $AlCl_4^-$ into the chain region will have an opposing effect and is clearly the dominant factor here.

In the crystalline phase, x-ray diffraction analysis[33,34] has shown the molecules to aggregate into ordered col-

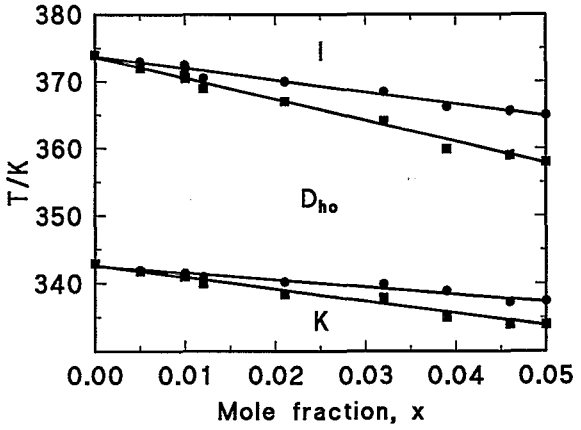


FIG. 2. Partial phase diagram of HAT6/$AlCl_3$ system determined by DSC, showing the isotropic phase $I$, the hexagonal columnar phase $D_{ho}$, and the crystalline phase $K$. All unlabeled areas are biphasic regions. The temperatures of the phase boundary curves are estimated to have errors of ±0.3 K.

umns, with the columns forming a hexagonal matrix. The intermolecular separation within the columns is equal to 0.354 nm. The axis-to-axis intercolumnar separation is 1.954 nm. In the columnar phase there is a relatively diffuse peak at 0.354 nm which corresponds to core–core scattering which can be clearly distinguished from the more liquidlike chain–chain scattering. It has been established[33] that in HAT6, the correlation length within the columns is of the order of 12 nearest neighbors and, therefore, that the columnar phase is of the type $D_{ho}$. No significant change in the scattering patterns was observed in either the crystalline or liquid crystalline phase, when the material was doped. In particular, no change in the intermolecular separation within the columns could be detected, indicating that the charge transfer induced by small quantities of $AlCl_3$, has only a minimal effect on the intermolecular separation. The incorporation of low concentrations of $AlCl_4^-$ ions without any appreciable change in crystal structure is possible because of the disorder within the side chain regions. Thus the most likely model for the structure of the doped $D_{ho}$ and $K$ phases, is one in which either $HAT6^{\cdot+}$ or $(HAT6)_n^{\cdot+}$ (Ref. 27) radical cations are incorporated into the triphenylene columns and the $AlCl_4^-$ anions into the hydrocarbon chain matrix.

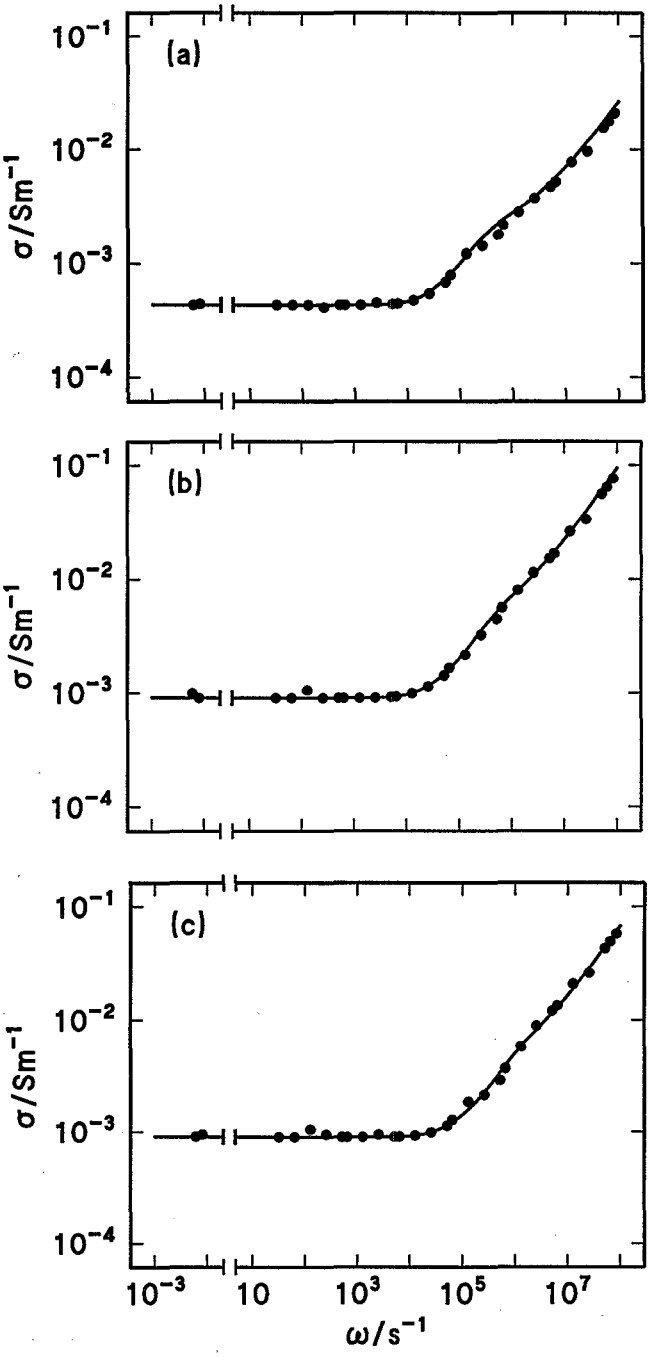


FIG. 3. Alternating current conductivity of HAT6/$AlCl_3$ ($x$=0.005) in unaligned phases. (a) The crystalline $K$ phase (320 K), (b) the liquid crystalline $D_{ho}$ phase (368 K), and (c) the isotropic phase (378 K). The solid lines represent the fitting of Eq. (14) with the parameters shown in Table IV.

### B. Electrical conductivity

Typical measurements of the frequency dependence of the conductivity for the unaligned samples, which are characterized by a spatially isotropic distribution of column directors, are given in Fig. 3. The general form of this behavior, with the conductivity being independent of frequency at low frequencies and becoming dependent on frequency at higher frequencies [$\sigma(\omega) \sim \omega^s$, $0 < s < 1$], is very similar to that observed in a broad range of structurally disordered materials,[35–39] and generally associated with charge transport occurring via a hopping or tunneling mechanism. This type of behavior can normally be explained in a straightforward manner in terms of a single charge carrier transport process.[35] A closer inspection of the data in Fig. 3, however, reveals that the frequency dependence is somewhat more complicated here: the behavior observed in the frequency-dependent region suggests the presence of more than one frequency-dependent charge transport process. With the objective of resolving these processes measurements have been made on aligned samples.

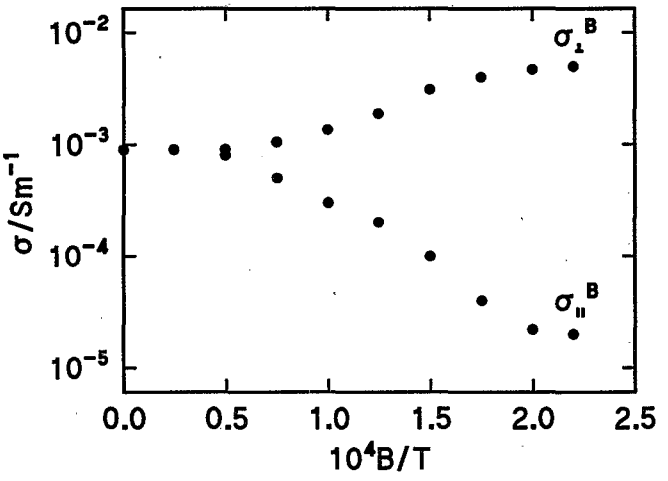


FIG. 4. Magnetic field dependence of the conductivity of HAT6/$AlCl_3$ ($x$=0.005, $f$=100 Hz) in the $D_{ho}$ phase at 368 K, prepared by slowly cooling from the isotropic to the columnar phase in the presence of the field. The field was switched off during the measurements.

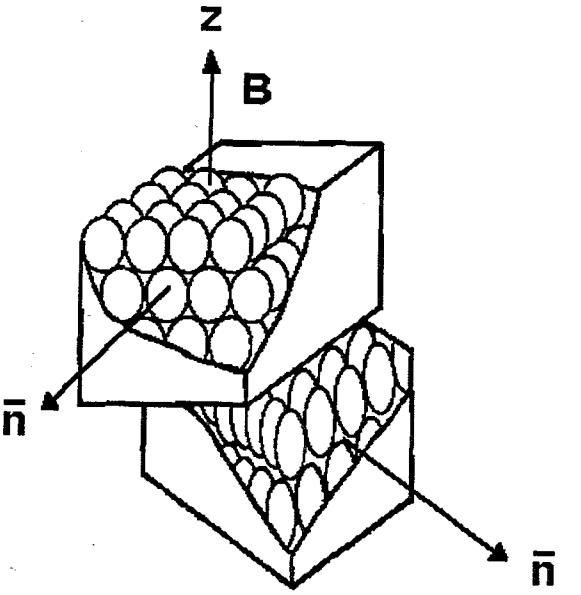


FIG. 5. A schematic diagram of the domain distribution obtained when a sample is slowly cooled in a strong magnetic field, $B$, along the $z$-direction. The $n$'s represent the domain directors, which are parallel to the column axes.

Aligned samples were prepared by slowly cooling from the isotropic phase into the columnar phase in the presence of a strong magnetic field. The conductivity of all samples aligned in this way became highly anisotropic, as shown for example in Fig. 4. The conductivity measured parallel to the direction of the aligning field is seen to be reduced with respect to that measured in the unaligned material, whilst that measured perpendicular to it is enhanced. The difference between these two values of the conductivity becomes constant for fields in excess of 2.0 T. The origin of this anisotropy can be understood in terms of the effect the magnetic field has on the alignment of the $D_{ho}$ phase. This phase has negative diamagnetic anisotropy, so that the column axes will tend to align in a direction perpendicular to that of the magnetic field as the phase nucleates from the isotropic melt. This results in a sample comprised of domains where column axes have a two-dimensional distribution of column axes in a plane perpendicular to the direction of the magnetic field,[29,40] as depicted in Fig. 5. Thus when the electric field is applied parallel to the direction of the magnetic field, charge carrier transport occurs in a direction perpendicular to the column axes. In contrast, when the electric field is applied perpendicular to the magnetic field direction, charge carrier transport occurs in directions both parallel and perpendicular to the column axes. However, this cylindrical distribution is well defined and provided that the individual domains are large enough to suppress grain boundary effects, the measured conductivity is the arithmetical average of the conductivities parallel $\sigma_{\parallel}$ and perpendicular $\sigma_{\perp}$ to the column axes.

Values of the conductivity measured parallel $\sigma_{\parallel}^{B}$ and perpendicular $\sigma_{\perp}^{B}$ to the direction of the magnetic field for samples aligned by slowly cooling from the isotropic phase into the columnar phase in the presence of a 2.2 T magnetic field are shown in Fig. 6. The values of $\sigma_{\parallel}^{B}$ and $\sigma_{\perp}^{B}$ are related simply to the conductivities parallel $\sigma_{\parallel}$ and perpendicular $\sigma_{\perp}$ to the column axes: $\sigma_{\parallel}^{B}=\sigma_{\perp}$ and $\sigma_{\perp}^{B}=\frac{1}{2}(\sigma_{\parallel}+\sigma_{\perp})$. This is, of course, assuming that the observed conductivities are governed solely by the intrinsic migration of charge carriers along and perpendicular to the columns. The fact that the plot of $\sigma_{\parallel}^{B}$ vs $\omega$ is consistent with a single process being involved suggests that this situation occurs. We have therefore identified $\sigma_{\parallel}^{B}$ with $\sigma_{\perp}$, and used this data to extract $\sigma_{\parallel}$ from $\sigma_{\perp}^{B}$. The results are presented in Fig. 7. We see that both $\sigma_{\parallel}$ and $\sigma_{\perp}$ appear to be governed by a single process in both the liquid crystalline and crystalline phases. Significantly, the orientational order of the columnar phase is seen to be frozen into the crystalline phase on cooling. Typically, $\sigma_{\parallel}\sim 10^3\,\sigma_{\perp}$, showing that conduction along the columns is strongly preferred.

The conductivity measured in the unaligned samples might be expected to correspond to the trace of the conductivity tensor, i.e., $\mathrm{tr}\{\sigma\}=\frac{1}{3}\sigma_{\parallel}+\frac{2}{3}\sigma_{\perp}$. However, we see that the low frequency limiting conductivity in Fig. 3(b), $\sim 1\times 10^{-3}$ S m$^{-1}$, is significantly smaller than the trace, $\sim 6\times 10^{-3}$ S m$^{-1}$, calculated from the data in Fig. 7(b), and is clearly dominated by a different process.

The variation of the low-frequency plateau values of $\sigma_{\parallel}$ and $\sigma_{\perp}$ with temperature, across all three phases is shown in Fig. 8. The temperature dependence in the crystalline phase is very weak; in the liquid crystalline phase it is more pronounced, yet still weak. Surprisingly the temperature dependence of the conductivity in the isotropic liquid phase is negative.

## IV. INTERPRETATION OF THE CONDUCTIVITY MEASUREMENTS

The form of the frequency dependence of the conductivities are indicative of charge carrier transport by a hop-

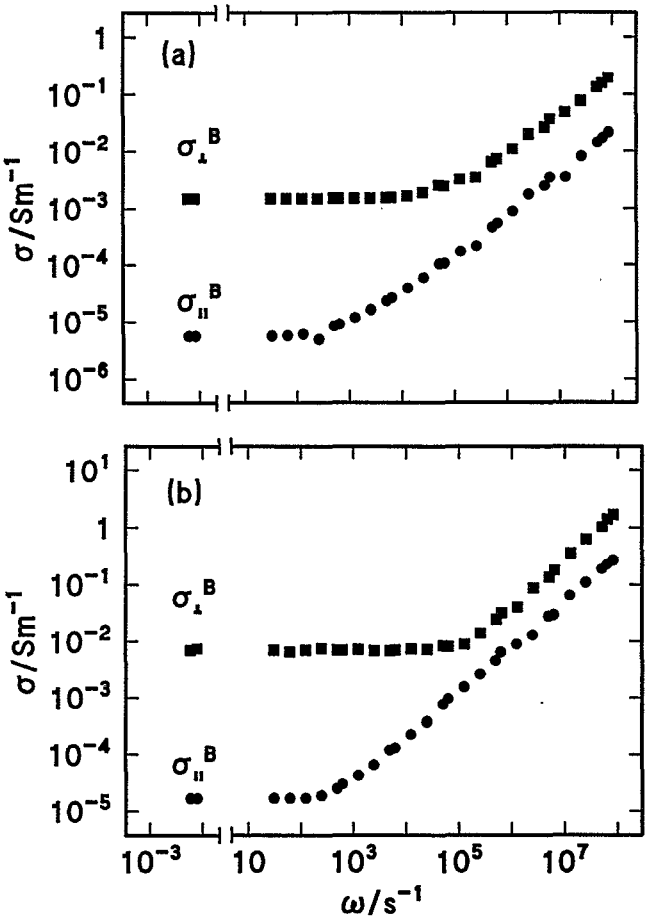


FIG. 6. Alternating current conductivities of macroscopically aligned samples of HAT6/$AlCl_3$ ($x=0.005$) after alignment in a magnetic field of 2.2 T in (a) the crystalline $K$ phase (320 K), (b) the liquid crystalline $D_{ho}$ phase (368 K), both parallel $\sigma_\parallel^B$ (●) and perpendicular $\sigma_\perp^B$ (■) to the field axis.

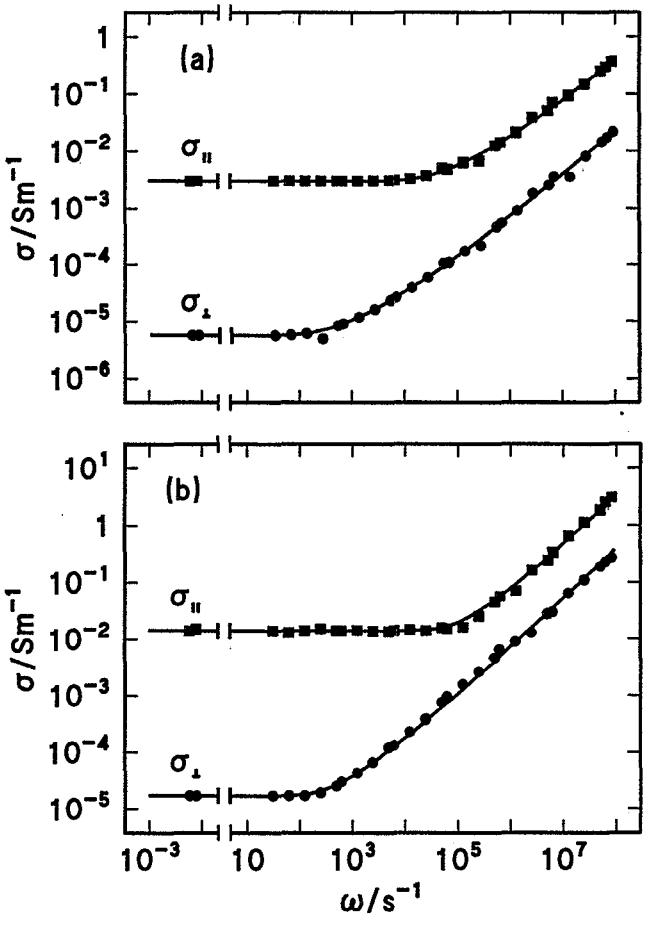


FIG. 7. Alternating current conductivities parallel $\sigma_\parallel$ (■) and perpendicular $\sigma_\perp$ (●) to the axes of the columns of HAT6/$AlCl_3$ ($x=0.005$) in (a) the crystalline $K$ phase (320 K) and (b) the liquid crystalline $D_{ho}$ phase (368 K). The solid lines represent the fitting of Eq. (12) with (a) $\lambda_\parallel=(5.0\pm0.1)\times10^4$, $\lambda_\perp=(5.0\pm0.1)\times10^2$, $\nu=-0.72\pm0.1$ (b) $\lambda_\parallel=(1.0\pm0.03)\times10^5$, $\lambda_\perp=(2.0\pm0.05)\times10^2$, $\nu=-0.79\pm0.1$.

ping mechanism. We have therefore analyzed the measurements using the Scher and Lax[41] model, introduced to analyze impurity conduction in amorphous semiconductors, and subsequently applied to variety of systems.[38,42,43] Scher and Lax developed the concept of the continuous time random walk (CTRW), first introduced by Montroll and Weiss,[44] in a form appropriate for describing charge transport in disordered materials. The frequency dependent diffusion coefficient $D(\omega)$ is given by

$$D(\omega)=\frac{\Delta_{\rm rms}^2}{2d}\cdot\frac{i\omega\Psi(i\omega)}{1-\Psi(i\omega)}, \tag{2}$$

where $\Delta_{\rm rms}^2$ is the mean-square displacement of the diffusing charge carriers, $d$ is the dimensionality of the system, and $\Psi(i\omega)$ is the Laplace transform of $\psi(t)$, the distribution function describing the probability for a hop to occur at time $t$ after the preceding one.

$\psi(t)$ determines the frequency dependence of the conductivity. If $\psi(t)$ has a finite first moment

$$\bar{t}=\int_0^\infty t\psi(t)dt, \tag{3}$$

then normal (Fickian) diffusion is observed. For example, for $\psi(t)$ of the form

$$\psi(t)=\lambda\exp(-\lambda t), \tag{4}$$

$$D(\omega)=(1/2d)\Delta_{\rm rms}^2\lambda \tag{5}$$

is obtained, where $\lambda$ is an arbitrary parameter and the mean hopping time $\bar{t}=1/\lambda$. Thus the diffusion coefficient, and the conductivity, which is related to the former by the generalized Nernst–Einstein equation,

$$\sigma(\omega)=(ne^2/kT)D(\omega) \tag{6}$$

are both independent of frequency.

If, on the other hand, the first moment of $\psi(t)$ diverges, then anomalous (non-Fickian) transport is obtained.[45] Of particular interest in this respect are $\psi(t)$ with long time tails, such as

$$\psi(t)=At^\nu/\Gamma(1+\nu),\quad 0>\nu>-1, \tag{7}$$

where $A$ is a constant, $\nu$ is an arbitrary parameter, and $\Gamma$ is the gamma function. In other words, the hopping proba-

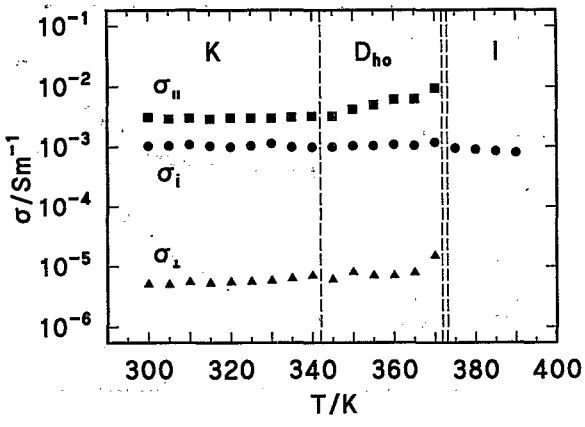


FIG. 8. The low frequency limiting conductivity ($f=100$ Hz) of HAT6/$AlCl_3$ ($x=0.005$) as a function of temperature.

bility is a slowly decaying function of time. Under these conditions, $\bar{\Delta}^2_{rms}$ becomes proportional to $t^{\nu}$ and $D(\omega)\sim\omega^{-\nu}$.

The conductivity in the HAT6/$AlCl_3$ system is independent of frequency at low frequencies and becomes dependent on frequency at higher frequencies. To model this type of frequency dependence requires an event time distribution which combines elements of both Eqs. (4) and (7), so as to produce a diffusion coefficient which crosses over from being frequency independent to frequency dependent. An appropriate functional form for $\psi(t)$, for which the first moment is finite, is

$$\psi(t)=\lambda(\lambda t)^{\nu}e^{-\lambda t}/\Gamma(\nu+1). \tag{8}$$

The Laplace transform of $\psi(t)$ is

$$\Psi(i\omega)=\mathcal{L}(\psi(t))=(1+i\omega/\lambda)^{-\nu-1} \tag{9}$$

and the diffusion coefficient is given by

$$D(\omega)=\frac{\Delta^2_{rms}}{2d}\cdot\frac{i\omega(1+i\omega/\lambda)^{-\nu-1}}{1-(1+i\omega/\lambda)^{-\nu-1}}. \tag{10}$$

The low frequency limit of Eq. (10) has the familiar form

$$D=\Delta^2_{rms}/2d\bar{t}. \tag{11}$$

Combining Eqs. (2) and (6) we obtain the following relationship for the frequency dependent conductivity:

$$\sigma(\omega)=\frac{ne^2}{kT}\cdot\frac{\Delta^2_{rms}}{2d}\cdot\frac{i\omega\Psi(i\omega)}{1-\Psi(i\omega)}, \tag{12}$$

which reduces, in the low frequency limit, to

$$\sigma(\omega)=\frac{ne^2}{kT}\frac{\Delta^2_{rms}}{2d}\lambda=\text{const}, \tag{13}$$

where $n$ is the concentration of charge carriers and $e$ the electronic charge. That is, at low frequencies, the system behaves as though it were an ordered system with just a *single* effective transfer rate between sites, $W_{eff}=\lambda\sim 1/\bar{t}$. This is a remarkable result and is not at all intuitively obvious. Though it is implicit in the analysis of Scher and Lax, its significance was subsequently highlighted by Bernasconi *et al.*[46] They showed that any distribution function $\psi(t)$ for which the first moment is finite, leads to such a relationship, so that the system exhibits an effective finite dc conductivity.

Equation (12) was fitted to the experimental data with $\nu$, $\lambda$, and $\Delta_{rms}$ as adjustable parameters, using the gradient expansion algorithm of Levenburg and Marquardt as described by Bevington.[47] The procedure required choosing initial values for the parameters $\nu$, $\lambda$, and $\Delta_{rms}$. The initial value of $\nu$ was determined from the slope of the frequency dependence at high frequencies (i.e., $\nu=-s$), and the initial value of $\lambda$ from the frequency where the conductivity crosses over from being frequency independent to frequency dependent. The initial value of $\Delta_{rms}$ was determined from $\lambda$ using Eq. (13), using values of $n$ calculated on the basis of Eq. (1) and $d=1$ for $\sigma_{\parallel}$ and $d=2$ for $\sigma_{\perp}$. The fitting of Eq. (12) was found to be quite robust, in that reliable convergence to the same solution did not depend critically on the initial parameter estimates. The values of the best fit parameters $\nu$ and $\lambda$ are given in Table I and those for the root mean hopping displacement $\Delta_{rms}$ in Table II for the $D_{ho}$ phase at 343 K.

### A. Aligned samples

The continuous lines in Figs. 7(a) and 7(b) represent the results of fitting Eq. (12) to the values of $\sigma_{\parallel}$ and $\sigma_{\perp}$. The agreement between experiment and Eq. (12) leads to the conclusion that the conductivity in aligned phases is governed by a single process. This process is the hopping of charge carriers between coulombic wells associated with the $AlCl_4^-$ counterions distributed along the molecular columns. This can be demonstrated by comparing values of the root-mean-square hopping displacement $\Delta_{rms}$ along the columns, with the mean distances $\Delta(x)$ between counterions along the columns, as calculated from the concentration $x$ of $AlCl_3$ assuming that the reaction represented in Eq. (1) goes to completion (Table II columns 1 and 4). Generally, there is good agreement between the corresponding values. Thus at low frequencies the conductivity is monitoring only the slowest motions (nonlocalized or long-range hops) of the charge carriers: fast motions (localized hops) do not contribute to the observed conductivity in the plateau region.

Using Eq. (1) and the conductivity equation $\sigma=ne\mu$, where $\mu$ is the charge carrier mobility, we are able to make estimates of the carrier mobility in the low frequency limit (Table III). Surprisingly, these mobilities are independent of concentration. That is, at a given temperature the charge carrier mobility appears to be determined by a single constant value of the diffusion coefficient, independent of the carrier concentration. In other words, in the low frequency limit, the system behaves as if it were an ordered system, displaying Fickian diffusion [Eq. (11)] with a single effective hopping rate between sites, but with this hopping rate $1/\bar{t}$ varying inversely with $\Delta^2_{rms}$ as the concentration of radical cations is varied.

TABLE I. Parameters $\lambda$ and $\nu$ obtained for the best fit of Eq. (12) to the conductivity data in the $D_{ho}$ phase at 343 K.

| $x$ | $10^5\ \lambda/s^{-1}$ parallel | $10^2\ \lambda/s^{-1}$ perpendicular | $\nu$ parallel | $\nu$ perpendicular |
|---|---|---|---|---|
| 0.005 | 0.69[a] | 1.54[a] | −0.790[b] | −0.721[b] |
| 0.009 | 2.89 | 8.66 | −0.792 | −0.726 |
| 0.01 | 3.46 | 15.5 | −0.795 | −0.719 |
| 0.012 | 3.73 | 21.5 | −0.791 | −0.720 |
| 0.05 | 35.4 | 48.8 | −0.792 | −0.720 |

Uncertainties
[a] ±3%.
[b] ±4%.

TABLE III. Conductivities and calculated mobilities as a function of concentration $x$ in the $D_{ho}$ phase of HAT6/$AlCl_3$ at 343 K.

| $x$ | $10^2\sigma_\parallel$ /$Sm^{-1}$ | $10^5\sigma_\perp$ /$Sm^{-1}$ | $10^8\mu_\parallel$ / $m^2V^{-1}s^{-1}$ | $10^{11}\mu_\perp$ / $m^2V^{-1}s^{-1}$ |
|---|---|---|---|---|
| 0.005 | 0.5 | 0.6 | 1.14 | 1.38 |
| 0.0099 | 1.0 | 1.2 | 1.15 | 1.38 |
| 0.010 | 0.9 | 1.1 | 1.02 | 1.25 |
| 0.012 | 1.2 | 1.33 | 1.14 | 1.26 |
| 0.050 | 5.0 | 5.32 | 1.14 | 1.21 |

## B. Unaligned samples

We are now in a position to attempt an analysis of the more complex frequency dependence observed in unaligned samples, Fig. 3. It is not explicable in terms of an average over an isotropic orientational distribution of "locally ordered" domains.This can be seen by examining the limiting low frequency conductivity in, for example, the $D_{ho}$ phase. This has the value $\sim 1\times10^{-3}$ S $m^{-1}$ which is considerably smaller than the calculated value of $6\times10^{-3}$ S $m^{-1}$, i.e., $\sigma_i < \frac{1}{3}\sigma_\parallel + \frac{2}{3}\sigma_\perp$ .

We have been able to model the data for the $K$ and $D_{ho}$ phases by assuming an isotropic distribution of ordered domains separated by grain boundaries, which themselves provide an alternative path for conduction.[48] However, the concept of grain boundaries is not tenable for the isotropic phase which exhibits the same conductivity behavior, and so we have sought a model which is applicable to all three phases.

Essentially, the observed behavior is considered to arise from the involvement of two distinct microscopic processes. One, which dominates the conductivity at low frequencies, is associated with the structural disorder in the unaligned material, and the other, which becomes apparent at higher frequencies, is associated with transport along molecular columns. To model this behavior, the observed frequency dependent diffusion coefficient has been taken to be a convolution of two frequency dependent diffusion coefficients, one for each of the two processes. $D(\omega)$ is now given by

$$D(\omega) = D_1(\omega) * D_2(\omega), \tag{14}$$

where the subscripts 1 and 2 denote the high and low frequency processes, respectively, and the $D_n$'s have the functional form of Eq. (10) with parameters $\lambda_n$, $\nu_n$, and $\Delta_n$ $(n=1,2)$.

Using Eqs. (6), (10), and (14) we are thus able to calculate the conductivity $\sigma(\omega)$ as a function of frequency. To fit this model to the experimental data for the $K$ and $D_{ho}$ phases [Figs. 3(a) and 3(b)] initial values of $\lambda_1$, $\nu_1$, and $\Delta_1$ have been taken to be those corresponding to $\sigma_\parallel$ for the macroscopically aligned $K$ and $D_{ho}$ phases. The initial value of $\lambda_2$ is estimated from the frequency at which the diffusion process changes from normal to anomalous, while $\Delta_2$ is estimated from $\lambda_2$ and the initial value of $\nu_2$ is set equal to $\nu_1$. Figure 3 shows examples of the fit of this model to the experimental data in all three phases. The values of the best fit parameters are given in Table IV.

The similarity of the values of $\Delta_1$ and $\lambda_1$ with the corresponding values of $\Delta_\parallel$ and $\lambda_\parallel$ for the $D_{ho}$ and $K$ phases leads to the identification of process "1" as being charge migration along molecular columns or stacks.The new and unexpected result is the similarity between the values of $\Delta_1$ and $\lambda_1$ for the $I$ phase at 378 K and the $D_{ho}$ phase at 368 K. This means that the conducting molecular stacks persist well into the isotropic liquid phase. The second process, which dominates the low frequency conductivity measurements must be associated with carrier transport between these supramolecular stacks. In other words, the charge carriers become trapped in molecular stacks of finite length. The distance $\Delta_2 \sim 200$ nm, or about 500 molecules, corresponds to the root-mean-square lengths of these stacks. It may seem surprising that these molecular stacks or "conduction pathways" can be so long in an isotropic liquid. However, it is important to realize that these pathways do not necessarily correspond to linear columns with fairly long persistence lengths as in the liquid crystalline phase, but only to contiguous face-to-face packing of triphenylene cores.

The continuity in behavior from the $I$ to the $D_{ho}$ phase and finally to the $K$ phase tells us that the mesoscopic structure of the $I$ phase must be "frozen in" as "defect structure" in the long-range order in the liquid crystalline and crystalline solid phases. The precise nature of these defects is not known at the present time. One possibility is that there exist "ion-pairs" in which an $AlCl_4^-$ ion is in direct contact with the face of a triphenylene core.[49] The fact that such defects are either absent or present in sub-

TABLE II. Mean charge carrier hopping distances $\Delta_{rms}$ obtained from the fitting of Eq. (12), and the mean separation of the counterions $\Delta(x)$ along the columns calculated using the stoichiometry of Eq. (1) for the $D_{ho}$ phase of HAT6/$AlCl_3$ at 343 K.

| $x$ | $\Delta_{rms}$/nm parallel | $\Delta_{rms}$/nm perpendicular | $\Delta(x)$/nm |
|---|---|---|---|
| 0.005 | 98.8[a] | 51.2[a] | 93.3 |
| 0.009 | 48.3 | 21.6 | 51.7 |
| 0.01 | 44.1 | 16.1 | 46.7 |
| 0.012 | 42.5 | 13.7 | 38.9 |
| 0.05 | 13.8 | 9.1 | 9.3 |

Uncertainties:
[a] ±3%.

TABLE IV. Best fit parameters for the conductivity measurements in Fig. 3 for unaligned HAT6/$AlCl_3$ in its $K$, $D_{ho}$ and $I$ phases.

| | $\Delta_1$/nm | $10^4\,\lambda_1/s^{-1}$ | $\nu_1$ | $\Delta_2$/nm | $10^3\,\lambda_2/s^{-1}$ | $\nu_2$ |
|---|---|---|---|---|---|---|
| $K$ (320 K) | 114[a] | 5.2[a] | −0.72[b] | 190[a] | 8.0[a] | −0.72[b] |
| $D_{ho}$ (368 K) | 87 | 8.8 | −0.79 | 183 | 20.0 | −0.79 |
| $I$ (378 K) | 86 | 9.0 | −0.81 | 178 | 21.2 | −0.81 |

Uncertainties:
[a]±3%.
[b]±4%.

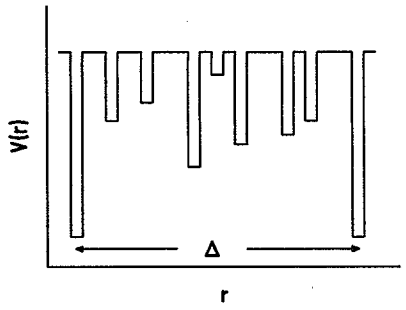


FIG. 9. A schematic diagram illustrating the potential $V(r)$ as *seen* by a charge carrier diffusing along a molecular column in the $D_{ho}$ phase.

stantially reduced concentrations in samples obtained by slowly cooling from the $I$ phase in a strong magnetic field suggests that they must be annealed out of the structure during domain growth. This confirms that they are non-equilibrium defects.

It is instructive to recognize the characteristic differences between the conductivity curves when two distinct processes are involved, as in Fig. 3, and when only a single tensorial process is involved but with an orientational distribution of the principal axes as in Fig. 6.

## V. DISCUSSION

It has been established that, in aligned samples the frequency dependence of the conductivity along the direction of the columns can be described in terms of a single charge transport process: hopping of the charge carriers between localized sites (radical cations) associated with the distribution of counterions along the molecular columns. Each counterion is associated with a given column in the structure, producing a localized site/coulombic well which is occupied by a charge carrier. It also must produce shallower wells on neighboring columns. Thus a charge carrier moving along a given column will *see* a potential which consists of relatively deep wells separated by a mean distance corresponding to the mean separation of the counterions (Table II), together with intervening shallower wells, associated with counterions on neighboring columns. A *typical* column potential is illustrated schematically in Fig. 9. A carrier in a deep well, can either migrate by tunneling to the next deep trap (direct tunneling) or absorb energy from the *lattice* and tunnel to a neighboring shallow trap (thermally assisted tunneling or under-barrier hopping). The former process is very unlikely because of the relatively great distances involved. We can see this by considering a square well potential, for which the transition probability $p_{ij}$ between sites is given by $p_{ij}\sim\nu\times\exp(-\gamma\Delta)$. So, for a 1 mole% sample, where $\Delta\sim44$ nm: using typical[50] values of $\nu\sim10^{12}$–$10^{14}$ $s^{-1}$ and $\gamma\sim10$ $nm^{-1}$, $p_{ij}\sim0$, that is, the transition probability is effectively zero.

At low frequencies/long times, where the conductivity is independent of frequency, the observed conductivity is governed by hopping between the deepest wells, whilst at high frequencies/short times, where the conductivity is frequency dependent, it is governed by hopping of carriers between localized, shallower wells. At higher frequencies still, and particularly in samples having a low concentration of $AlCl_3$, we might expect to observe charge migration between individual HAT6 molecules uninfluenced by coulombic fields from nearby counterions. Since this process is expected to have a single transition rate, the maximum transition rate for the system, we would expect the conductivity to display a high frequency plateau.[41] Experiments are currently in progress to establish the high frequency conductivity behavior.

It is instructive to compare this classical picture of charge transport with its equivalent band-structure picture. In discotic liquid crystals, just as in molecular crystals, overlap of $\pi$ orbitals leads to the formation of energetically closely spaced but spatially delocalized, electronic energy levels (electronic bands). The highest occupied electronic levels constitute the valence band (VB) and the lowest unoccupied levels, the conduction band (CB). The width of the band gap $E_g$, between the VB and CB, determines the intrinsic electronic properties of the material. An intrinsic semiconductor, for example, is characterized by a small band gap and a low density of highly mobile charge carriers. In the commonly observed $D_{ho}$ and $D_{hd}$ mesophases of many discotic liquid crystals, the lack of true long range positional order within the columns leads to large bandgaps, so that these materials are intrinsically insulating.

Initially, the conductivity increase observed on doping HAT6 with $AlCl_3$ was considered to result from the formation of unfilled electronic bands.[4] It was simply assumed that upon $p$-type doping, electrons were removed from the top of the VB, in analogy to the mechanism of generation of charge carriers in doped inorganic semiconductors, and that the electrical conductivity arises from the migration of these positive holes in the VB. However, the low value of the charge carrier mobility and the observed frequency dependence of the conductivity militate against this interpretation.

More realistically, since for organic molecules in general, the equilibrium geometry in the ionized state is usually different from that in the ground state,[51] we can expect that doping of HAT6 with Lewis acids gives rise to polarons, radical cations associated with a lattice deformation and the presence of localized states in the band gap,[52] as illustrated schematically in Fig. 10. Conduction by polarons is believed to be the dominant process in conjugated

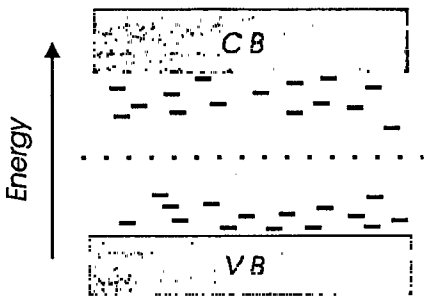


FIG. 10. A schematic band diagram for the HAT6/$AlCl_3$ system. The shaded regions represent the valence (VB) and conduction bands (CB). The localized states are represented by the short line segments at the edges of the bands.

polymers with nondegenerate ground states, such as polypyrrole. In this system, the polarons appear to extend over about four pyrrole rings.[53] At present we are uncertain as to the exact nature of the polarons in the present system, but both optical and ESR experiments are in progress to characterize their nature. The charge transport process occurs because of the strong carrier-phonon interaction: the localized hole tunnels from site to site by interactions with vibrational modes.

In the unaligned phases two frequency-dependent charge-transport processes have been identified: one, which dominates at high frequencies, has been identified with charge migration along molecular columns as in aligned samples, and the other, which dominates at low frequencies, has been identified with structural defects. In aligned phases, the coherence length of the columns appears to be effectively infinite and there are no apparent barriers to the long range migration of charge. This appears to be no longer the case in the unaligned phases. Instead, it appears that the coherence lengths of the molecular stacks are now finite, of the order of 200 nm. These stacks shorten with increasing temperature in the isotropic liquid phase, but do not vary significantly with temperature in either the $D_{ho}$ or $K$ phases. The low frequency conductivity process is, we believe, associated with the transport of charge between these mesoscopic column elements. The mesoscopic structure of the isotropic liquid phase appears to be "frozen-in" as a "defect structure" into the liquid crystalline and crystalline phases on cooling.

This interpretation is in direct contradiction to the results of Schouten *et al.*[23] They studied charge migration in supramolecular stacks of peripherally substituted porphyrins using a radiation induced microwave conductivity technique.[54] This involves ionization to form electron-hole pairs which become localized within the cores of separate (neighboring) columns. In the crystalline and liquid crystalline phases high conductivities are observed, but in the isotropic melt phase the conductivity is dramatically reduced. They conclude therefore, that the supramolecular structural organization of the crystalline and liquid crystalline phases is essential for conductivity and that this is missing in the isotropic melt phase. This is in apparent contradiction to the results reported here! Our experiments are sensitive to charge migration along single-column elements which clearly seem to persist well into the liquid phase. In contrast, the migration of electron-hole pairs requires, at least, pairs of collinear columns. Thus both observations can only be reconciled by postulating the existence of fairly long molecular stacks, but the absence of any significant orientational correlations of these stacks.

The temperature dependence of the conductivity, Fig. 8, can now be understood in terms of the effect of temperature on the distribution of counterions and the coulombic wells that they give rise to. The strong increase of $\sigma_{\|}$ with temperature in the $D_{ho}$ phase must be a consequence of the relaxation of the structure which is effectively frozen-in in the crystalline solid phase giving rise to the much weaker temperature dependence of $\sigma_{\|}$ in that phase. Thus studies of the effect of temperature on the intrinsic charge transport process can only be realistically made on such *glassy* solid states, where temperature dependent relaxation of the structure is greatly diminished. The temperature dependence in the isotropic phase may be understood qualitatively in terms of the effect of temperature on the length of the molecular stacks which decreases with increasing temperature.

The results presented in this paper have emphasized the importance of charge transport studies on well aligned liquid crystalline and crystalline solid phases. The charge transport process in unaligned phases is dominated by the mesoscopic disorder "frozen-in" from the isotropic liquid phase. Such defects appear to be absent in aligned samples. The importance of producing aligned phases has been recognized by other workers,[7] but to our knowledge we are the first to report measurements on such samples and thereby obtain a plausible interpretation of the conduction process. In turn, this emphasizes the importance of retaining the mesophase behavior. Doping with small quantities of electron acceptors (or donors) preserves the mesophase behavior: creating charge transfer or radical-ion salts suppress it. Drenth *et al.*[6] oxidized HAT6 with 70 mole% of $I_2$, but were unable to observe any anisotropy in the conductivity. The level of conductivity that they measured was of the same order of magnitude as that observed by us using much smaller quantities of dopant. There is, however, an alternative approach to the production of aligned crystalline (but not liquid crystalline) conductors: this makes use of the alignment properties of liquid crystals. Safinya *et al.*[5] have produced highly oriented fibres of crystalline HAT5 by drawing strands from the $D_{ho}$ phase and then made charge transfer salts by exposing these strands to bromine vapor.

With regard to the objective of producing quasi-one-dimensional conductors, the preferred mechanism of conduction along the column axes must be in electronic bands. For instance, in the TCNQ charge transfer complexes, the conductivity in the molecular stacking (b) direction is due to charge transport in electronic bands, but in the a-direction, where the charge goes between unlike molecules, it is due to hopping. Consequently, conductivity an-

isotropies of 30 000 are typical. Organic polymers offer another route to quasi-one-dimensional conductors. Polyacetylene, for instance, can be stretched in one direction and shows considerable anisotropy in electrical and optical properties as a result. For polyacetylene doped with $AsF_5$, after stretching by a factor of 3, the anisotropy of conductivity $\sim 16$, with $\sigma_{\parallel} \sim 20$ S m$^{-1}$ along the stretch direction.[55]

Despite the limitation of charge transport by hopping, liquid crystalline conductors do, however, offer a distinct advantage over other types of molecular conductor in that their macroscopic alignment is easily manipulable with magnetic fields or by suitable surfaces. In contrast, the anisotropy of crystalline organic conductors is fixed when the materials crystallize, and in organic polymers it can only be changed by mechanical treatment, such as stretching or drawing. Another attractive feature is the freedom to vary (within limits) the concentration of dopant. This is far more difficult in crystalline complexes due to crystallographic constraints.

Finally, we address the issue of the contribution of the $AlC_4^-$ counterions, to the conductivity. The fact that these ions are situated in the disordered or liquidlike chain region leads one to expect such a contribution, at least in principle. There is however, no indication in the conductivity measurements of such a contribution. This would be evident as a rapid fall in $\sigma$ at low frequencies due to space-charge limitation effects at the electrodes. This suggests that the counterions are essentially immobilized, or that their contribution to the conductivity is very much smaller than that due to electron migration. An upper limit to this contribution can be estimated by calculating the diffusion coefficient of $AlCl_4^-$ ions in a liquid hydrocarbon with the viscosity of liquid *n*-hexane at the same temperature. Using the Stokes–Einstein equation $D=kT/6\pi\eta r$, where $\eta$(0.3 poise) is the kinematic viscosity of *n*-hexane at temperature $T$(298 K), and $r$(0.3 nm) is the radius of the diffusing ion, we estimate the diffusion coefficient of $AlCl_4^-$ ions in *n*-hexane to be $D \sim 2.5\times10^{-11}$ m$^2$ s$^{-1}$. This compares with the measured diffusion coefficient $D_{\parallel} = 3.4\times10^{-10}$ m$^2$ s$^{-1}$ in the $D_{ho}$ phase of a 1 mole% $AlCl_3$ doped sample at the same temperature. In practice, the diffusivity of the $AlCl_4^-$ ion is expected to be less than this since we have used a minimum estimate of the ionic radius, and the viscosity of the fixed alkoxy side-chains is likely to be considerably greater than that for *n*-hexane. Since this level of diffusivity would make a significant contribution to the overall conductivity, it would appear that the counterions are effectively immobilized in the side-chain region presumably due to Coulombic interaction with neighboring radical cations. Likewise, lateral diffusion of the cations between columns could also contribute to $\sigma_{\perp}$, since in HAT8 at 333 K $D_{\perp} \sim 5\times10^{-11}$ m$^2$ s$^{-1}$.[56] But again there is no indication of ionic diffusion, presumably because the cations are immobilized within the columns.

## VI. CONCLUSIONS

The ac conductivity of HAT6 doped with small quantities of $AlCl_3$ has been studied as a function of frequency, temperature and concentration of $AlCl_3$, in the isotropic liquid, liquid crystalline and crystalline phases. The most important findings can be summarized as follows:

- HAT6 when doped with small quantities of $AlCl_3$ is converted from an insulator to a quasi-one-dimensional semiconductor with the column axes being the preferred direction of charge transport.
- The $D_{ho}$ phase can be macroscopically aligned by cooling from the isotropic melt phase in a strong magnetic field, in excess of 2T. This alignment, and hence the anisotropy of conductivity, are frozen into the crystalline solid phase on further cooling.
- The frequency dependence of the conductivity, as measured along the direction of the columns in aligned phases, can be described in terms of a single charge transport process in which the charge carriers hop between localized sites (radical cations) associated with $AlCl_4^-$ counterions linearly distributed off-axis along the columns.
- The charge carrier diffusion coefficient is independent of the concentration of dopant ($0<x<0.05$) and has the value $D_{\parallel} \sim 3.4\times10^{-10}$ m$^2$ s$^{-1}$.
- The corresponding charge carrier diffusion coefficient in the direction perpendicular to the column axes has a value $D_{\perp} \sim 5\times10^{-13}$ m$^2$s$^{-1}$, some three orders of magnitude smaller.
- Charge transport proceeds stochastically, by phonon-assisted tunneling between neighboring Coulombic wells.
- In the isotropic melt phase, the conductivity measurements reveal the persistence of molecular stacks some 200 nm in length. The mesoscopic structure of the isotropic melt phase seems to be "frozen-in" as a "defect structure" of the liquid crystalline and subsequent crystalline solid phase on cooling.

The results presented in this paper provide an insight into the relationship between the microscopic molecular structure and the conductivity of this new class of quasi-one-dimensional conductors. There are now the prospects of being able to explore this relationship in greater detail: for example, what are the effects of ring structure, side-chain length, nature and concentration of dopant, and disorder?

## ACKNOWLEDGMENTS

We wish to thank Professors M. J. Pilling and M. A. Anisimov and Dr. G. V. Buxton for helpful discussions, and the Science and Engineering Research Council and British Technology Group Ltd. for financial support of this work.

[1] I. A. Howard, in *Semiconductors and Semimetals Vol. 27, Highly Conducting Quasi-One-Dimensional Organic Crystals*, edited by E. Conwell (Academic, London, 1988).

[2] H. Schultz, H. Lehmann, M. Rein, and M. Hanack, *Structure and Bonding*, **74**, 41 (1991); T. J. Marks, Angew. Chem. Int. Ed. Engl. **29**, 857 (1990); A.-M. Giroud-Godquin and P. M. Maitlis, *ibid.* **30**, 375 (1991).

[3] *Handbook of Conducting Polymers*, edited by T. A. Skotheim (Marcel Dekker, New York, 1986), Vols. I and II.

[4] N. Boden, R. J. Bushby, J. Clements, M. V. Jesudason, P. F. Knowles, and G. Williams, Chem. Phys. Lett. **152**, 94 (1988); *ibid.* **154**, 613 (1989).

[5] L. Y. Chiang, J. P. Stokes, C. R. Safinya, and A. N. Bloch, Mol. Cryst. Liq. Cryst. **125**, 279 (1985).
[6] J. van Keulen, T. W. Warmerdam, R. J. M. Nolte, and W. Drenth, Recl. Trav. Chim. Pays-Bas. **106**, 534 (1987).
[7] G. B. M. Vaughan, P. A. Heiney, J. P. McCauley, Jr., and A. B. Smith III, Phys. Rev. B **46**, 2787 (1992).
[8] J. Ferraris, D. O. Cowan, and V. Walat Ka, Jr., J. Am. Chem. Soc. **95**, 948 (1973).
[9] J. S. Miller, Ann. N.Y. Acad. Sci. **313**, 25 (1978); L. C. Isett and E. A. Peruz-Albuerne, Ann. N.Y. Acad. Sci. **313**, 395 (1978).
[10] L. B. Schein and D. W. Brown, Mol. Cryst. Liq. Cryst. **87**, 1 (1982).
[11] B. A. Scott, S. J. LaPlaca, J. B. Torrance, B. B. Silverman, and B. Welber, Ann. N.Y. Acad. Sci. **313**, 369 (1978).
[12] E. M. Conwell and N. C. Banik, Mol. Cryst. Liq. Cryst. **79**, 95 (1982).
[13] M. J. Cohen, L. B. Coleman, A. F. Garito, and A. J. Heeger, Phys. Rev. B **10**, 1298 (1974).
[14] K. Bechgaard, C. S. Jacobsen, K. Mortensen, H. J. Pedersen, and N. Thorup, Solid State Commun. **33**, 1119 (1980); K. Mortensen, Synth. Met. **9**, 63 (1984).
[15] C. S. Jacobsen, D. B. Tanner, and K. Bechgaard, Phys. Rev. Lett. **46**, 1142 (1981).
[16] C. J. Schramm, R. P. Scaringe, D. R. Stojakovic, B. M. Hoffman, J. A. Ibers, and T. J. Marks, J. Am. Chem. Soc. **102**, 6702 (1980).
[17] J. S. Miller and A. J. Epstein, Prog. Inorg. Chem. **20**, 1 (1976); J.R. Ferraro, Coord. Chem. Rev. **43**, 205 (1982); T. E. Phillips, R. P. Scarenge, B. M. Hoffman, and J. A. Ibers, J. Am. Chem. Soc. **102**, 3435 (1980).
[18] S. Konoshi, M. Hoshino, and M. Imamura, J. Phys. Chem. **84**, 3437 (1980); G. P. Fulton and G. N. La Mar, J. Am. Chem. Soc. **98**, 2119 (1980); A. Ulman, J. Manassen, F. Frolow, and D. Rabinovich, Inorg. Chem. **20**, 1987 (1981).
[19] J. M. Williams, A. J. Schultz, A. E. Underhill and K. Carneiro, in *Extended Linear Chain Compounds,* Vol. I, edited by J. S. Miller (Plenum, New York, 1982), p. 73.
[20] D. J. Wood, A. E. Underhill, A. J. Schultz, and J. M. Williams, Solid State Comm. **30**, 501 (1979).
[21] S. Chandrasekhar and G. S. Ranganath, Rep. Prog. Phys. **53**, 57 (1990).
[22] J. Simon and C. Sirlin, Pure Appl. Chem. **61**, 1625 (1989); C. Piechocki, J. Simon, A. Skoulios, D. Guillon, and P. Weber, J. Am. Chem. Soc. **104**, 5245 (1982).
[23] B. A. Gregg, M. A. Fox, and A. J. Bard, J. Am. Chem. Soc. **111**, 3024 (1989); P. G. Schouten, J. M. Warman, M. P. de Haas, M. A. Fox, and H.-L. Pan, Nature **353**, 736 (1991); S. Gaspard, P. Maillard, and J. Billard, Mol. Cryst. Liq. Cryst. **123**, 369 (1985).
[24] V. Gionis, H. Strzelecka, M. Veber, R. Kormann, and L. Zuppiroli, Mol. Cryst. Liq. Cryst. **137**, 365 (1986).
[25] J. F. van der Pol, E. Neelman, J. W. Zwicker, R. J. M. Nolte, W. Drenth, J. Aerts, R. Visser, and S. J. Picken, Liq. Cryst. **6**, 577 (1989).
[26] Z. Belarbi, C. Sirlin, J. Simon, and J. J. Andre, J. Phys. Chem. **93**, 8105 (1989).
[27] N. Boden, R. Borner, D. R. Brown, R. J. Bushby, and J. Clements, Liq. Cryst. **11**, 325 (1992).
[28] N. Boden, R. J. Bushby, L. Ferris, C. Hardy, and F. Sixl, Liq. Cryst. **1**, 109 (1986).
[29] D. Goldfarb, Z. Luz, and H. Zimmerman, J. Phys. **42**, 1303 (1981).
[30] C. Destrade, M. C. Mondon, and J. Malthête, J. Phys. Colloq. **40**, C3-18 (1979).
[31] D. E. Martire, in *The Molecular Physics of Liquid Crystals,* edited by G.R. Luckhurst and G. W. Gray (Academic, New York, 1987), p. 239.
[32] R. Borner, Ph.D. thesis, Leeds University, Leeds, U.K., 1992.
[33] C. R. Safinya, N. A. Clark, K. S. Liang, W. A. Varady, and L. Y. Chiang, Mol. Cryst. Liq. Cryst. **123**, 205 (1985); L. Y. Chiang, C. R. Safinya, N. A. Clark, K. S. Liany, and A. N. Bloch, J. Chem. Soc. Chem. Commun. 695 (1985).
[34] N. Boden, R. J. Bushby, and J. Clements (unpublished results).
[35] H. Bottger and V. V. Bryskin, *Hopping Conduction in Solids* (VCH, Berlin, 1985).
[36] N. F. Mott and E. A. Davies, *Electronic Processes in Non-Crystalline Materials* (Clarendon, Oxford, 1979).
[37] M. Pollak and T. H. Geballe, Phys. Rev. **122**, 1742 (1961); M. Abkowitz, D. F. Blossey, and A. I. Lakatos, Phys. Rev. B **12**, 3400 (1975).
[38] A. J. Epstein, H. Rommelman, M. Abkowitz, and H. W. Gibson, Mol. Cryst. Liq. Cryst. **77**, 81 (1981).
[39] J. Simon and J.-J. Andre, *Molecular Semiconductors* (Springer-Verlag, Berlin, 1985).
[40] G. Sigaud, M. F. Archard, C. Destrade, and N. H. Tinh, in *Liquid Crystals of One and Two Dimensional Order,* edited by W. Helfrich and G. Heppke (Springer-Verlag, Berlin, 1980), p. 403.
[41] H. Scher and M. Lax, Phys. Rev. **7**, 4491 (1973); *ibid.* **7**, 4502 (1973).
[42] M. Abkowitz, A. Lakatos, and H. Scher, Phys. Rev. B **9**, 1813 (1974); A. R. Long, Adv. Phys. **31**, 553 (1982).
[43] H. Kahnt and F. Schirrmeister, J. Non-Cryst. Solids **90**, 421 (1987).
[44] E. W. Montroll and G. H. Weiss, J. Math. Phys. **6**, 167 (1965).
[45] H. Scher and E. W. Montroll, Phys. Rev. B **12**, 2455 (1975).
[46] J. Bernasconi, W. R. Schneider, and W. Wyss, Z. Phys. B **37**, 175 (1980); S. Alexander, J. Bernasconi, W. R. Schneider, and R. Orbach, Rev. Mod. Phys. **53**, 175 (1981).
[47] P. R. Bevington, *Data Reduction and Error Analysis for the Physical Sciences* (McGraw-Hill, London, 1969).
[48] N. M. Beekmans and L. Heyne, Electrochim. Acta. **21**, 303 (1976); J. R. Macdonald, *Impedance Spectroscopy* (Wiley, New York, 1987).
[49] R. J. Bushby and H. L. Steel, J. Chem. Soc. Perkin Trans. **2**, 1169 (1990).
[50] J. V. Beitz and J. R. Miller, J. Chem. Phys. **71**, 4579 (1979).
[51] R. H. Baughmann, J. L. Brédas, R. R. Chance, R. L. Elsenbaumer, and L. W. Shacklette, Chem. Rev. **82**, 209 (1982).
[52] J. Brédas and G. B. Street, Acc. Chem. Res. **18**, 309 (1985).
[53] J. L. Brédas, J. C. Scott, K. Yakushi, and G. B. Street, Phys. Rev. B **30**, 1023 (1984).
[54] J. M. Warman and M. P. de Haas, Radiat. Phys. Chem. **34**, 581 (1989).
[55] Y. W. Park, M. A. Druy, C. K. Chiang, A. G. MacDiarmid, A. G. Heeger, H. Shirakawa, and S. Ikeda, J. Polym. Sci. Polym. Lett. **17**, 195 (1979); S. Roth, H. Bleier, and W. Puckacki, Faraday Discuss. Chem. Soc. **88**, 223 (1989).
[56] R. Y. Dong, D. Goldfarb, M. E. Moseley, Z. Luz, and H. Zimmerman, J. Phys.Chem. **88**, 3148 (1984).